

a normal thymus, a single peptide does not select millions of different TCRs, as has been suggested in the analyses of H-2M knockout and A^bEp mice (3, 4). Instead, the signal through the TCR that eventually leads to positive selection is driven by and dependent on specific interactions with self peptides. This degree of selectivity may be similar to the recognition of peptide during T cell activation. Indeed, it would be reasonable for the immune system to evaluate T cells during development on the basis of the rules of recognition that are required in the periphery.

The specific recognition of peptides appears so central to the generation of a complete T cell repertoire that even peptides present at very low levels can contribute to positive selection of T cells. These peptides generate the bulk of the diversity within MHC-bound peptides and probably support the development of the majority of selected thymocytes. This requirement for diverse, low-abundance peptides suggests that specificity during positive selection is fundamental to the generation of a broad, functional T cell repertoire.

References and Notes

1. M. J. Bevan, *Immunity* **7**, 175 (1997); P. J. Fink and M. J. Bevan, *Adv. Immunol.* **59**, 99 (1995); G. Anderson, N. C. Moore, J. J. Owen, E. J. Jenkinson, *Annu. Rev. Immunol.* **14**, 73 (1996); B. J. Fowlkes and E. Schweighoffer, *Curr. Opin. Immunol.* **7**, 188 (1995); C. J. Guidos, *ibid.* **8**, 225 (1996); C. Benoist and D. Mathis, *ibid.* **9**, 245 (1997); P. Marrack and J. Kappler, *ibid.*, p. 250.
2. K. A. Hogquist, M. A. Gavin, M. J. Bevan, *J. Exp. Med.* **177**, 1469 (1993); P. G. Ashton-Rickardt, L. Van-Kaer, T. N. Schumacher, H. L. Ploegh, S. Tonegawa, *Cell* **73**, 1041 (1993); K. A. Hogquist et al., *ibid.* **76**, 17 (1994); P. G. Ashton-Rickardt et al., *ibid.*, p. 651; E. Sebzda et al., *Science* **263**, 1615 (1994); K. A. Hogquist et al., *Immunity* **6**, 389 (1997); Q. Hu et al., *ibid.* **7**, 221 (1997).
3. L. Ignatowicz et al., *Immunity* **7**, 179 (1997); C. D. Surh, D. S. Lee, W. P. Fung-Leung, L. Karlsson, J. Sprent, *ibid.*, p. 209.
4. S. Tourne et al., *ibid.*, p. 187;
5. W. P. Fung-Leung et al., *Science* **271**, 1278 (1996); W. D. Martin et al., *Cell* **84**, 543 (1996); T. Miyazaki et al., *ibid.*, p. 531.
6. L. Ignatowicz, J. Kappler, P. Marrack, *Cell* **84**, 521 (1996);
7. C. E. Grubin, S. Kovats, P. deRoos, A. Y. Rudensky, *Immunity* **7**, 197 (1997).
8. G. M. Barton and A. Y. Rudensky, *Int. Immunol.* **10**, 1159 (1998).
9. The li-pEα construct has been described elsewhere (8). To generate transgenic mice, we injected purified li-pEα DNA into (B6 × DBA/2) F₁ × liKO embryos. Integration into the mouse germ line was assessed by polymerase chain reaction amplification of tail DNA from the progeny of transgenic founders, with primers specific for the li-pEα transgene.
10. G. M. Barton and A. Y. Rudensky, data not shown.
11. L. Denzin, personal communication.
12. S. Tourne et al., *Proc. Natl. Acad. Sci. U.S.A.* **94**, 9255 (1997).
13. S. Kovats et al., *J. Exp. Med.* **187**, 245 (1998).
14. G. M. Barton and A. Y. Rudensky, data not shown.
15. Mixed lymphocyte cultures were performed with C57BL/6 (H-2^b), BALBc (H-2^d), Tg:li^{KO}, and Tg:dbl^{KO} splenocytes and lymph node cells. Irradiated (20 Gy) splenocyte stimulator cells (4 × 10⁵ or 2 × 10⁵) were cultured with 4 × 10⁵ lymph node responder cells in each pairwise combination of the four mouse types. After 3 days, the cultures were pulsed with 0.5

- μCi of ³H-thymidine for 1 day, harvested, and thymidine incorporation was measured. Both Tg:li^{KO} and Tg:dbl^{KO} lymph node cells developed significant proliferative responses to C57B/6 stimulators.
16. T cell-depleted bone marrow cells (3.5 × 10⁶) from AND (20), Tcli (27), and TEa (7) TCR transgenic mice were injected intravenously into irradiated Tg:li^{KO} mice. These TCRs are specific for PCC(81-104)-I-E^k, human CLIP(85-101)-I-A^b, and Eα(52-68)-I-A^b complexes, respectively. Thymocytes and splenocytes were stained for CD4, CD8, and TCR and analyzed by flow cytometry. Small numbers of CD4 thymocytes, as well as peripheral CD4 T cells, in Tcli→Tg:li^{KO} and AND→Tg:li^{KO} chimeric mice indicated that both of these TCRs cannot be selected on Tg:li^{KO} thymic epithelium. Furthermore, as expected, TCR transgenic T cells in TEa→Tg:li^{KO} chimeras were deleted.
17. D. B. Murphy et al., *Nature* **338**, 765 (1989).
18. A. Y. Rudensky, S. Rath, P. Preston-Hurlburt, D. B. Murphy, C. A. Janeway Jr., *ibid.* **353**, 660 (1991); A. Y. Rudensky, unpublished observations.
19. H. Pircher, U. H. Rohrer, D. Moskophidis, R. M. Zinkernagel, H. Hengartner, *Nature* **351**, 482 (1991); J. Yagi and C. A. Janeway Jr., *Int. Immunol.* **2**, 83 (1990); K. A. Hogquist, S. C. Jameson, M. J. Bevan, *Immunity* **3**, 79 (1995).
20. J. Kaye et al., *Nature* **341**, 746 (1989).

21. P. Wong and A. Y. Rudensky, in preparation.
22. M. Liljedahl et al., *Immunity* **8**, 233 (1998).
23. Erythrocyte-depleted splenocytes were analyzed for expression of MHC class II molecules. Cells were incubated on ice with biotinylated mAbs Y3P (I-A^b, American Type Culture Collection HB183), YAe (pEα-I-A^b) (17), and 15G4 [CLIP-I-A^b (22)], followed by streptavidin-fluorescein isothiocyanate (FITC) (Vector). Stained cells were analyzed by a FACScan flow cytometer (Becton-Dickinson).
24. Thymocytes or erythrocyte-depleted splenocytes were incubated on ice with anti-CD4-phycoerythrin, anti-CD8α-FITC, and anti-TCRβ-biotin mAbs (all from Pharmingen) followed by streptavidin-Tricolor (Caltag). Stained cells were analyzed by a FACScan flow cytometer (Becton-Dickinson).
25. We thank A. W. Goldrath for helpful discussions and advice, M. J. Bevan and P. J. Fink for comments on the manuscript, S. Eastman for technical assistance, C. Wilson for generation of transgenic mice, and D. Wilson for maintenance of mice. Care of all experimental animals was in accordance with the guidelines of the University of Washington. Supported by a Hall-Ammerer Memorial Fellowship (G.M.B.), the NIH (A.Y.R.), and the Howard Hughes Medical Institute (A.Y.R.).

7 October 1998; accepted 30 November 1998

Blockade of NMDA Receptors and Apoptotic Neurodegeneration in the Developing Brain

Chrysanthy Ikonomidou,* Friederike Bosch, Michael Miksa, Petra Bittigau, Jessica Vöckler, Krikor Dikranian, Tanya I. Tenkova, Vanya Stefovskaja, Lechoslaw Turski, John W. Olney

Programmed cell death (apoptosis) occurs during normal development of the central nervous system. However, the mechanisms that determine which neurons will succumb to apoptosis are poorly understood. Blockade of N-methyl-D-aspartate (NMDA) glutamate receptors for only a few hours during late fetal or early neonatal life triggered widespread apoptotic neurodegeneration in the developing rat brain, suggesting that the excitatory neurotransmitter glutamate, acting at NMDA receptors, controls neuronal survival. These findings may have relevance to human neurodevelopmental disorders involving prenatal (drug-abusing mothers) or postnatal (pediatric anesthesia) exposure to drugs that block NMDA receptors.

Glutamate promotes certain aspects of neuronal development, including migration, differentiation, and plasticity (1). In the first 2 weeks of neonatal life in the rat, the NMDA

subtype of glutamate receptor undergoes a period of hypersensitivity, in which neurons bearing NMDA receptors are rendered highly sensitive to excitotoxic degeneration (2). During this period, NMDA receptors are primary mediators of glutamatergic fast excitatory neurotransmission in the brain (3). Although NMDA receptor activation can promote survival of cerebellar granule cells in vitro (4) or dentate granule neurons in vivo (5), evidence that even transient inactivation of NMDA receptors can be lethal for many neurons has not been described. We now report that during a specific stage in ontogenesis coinciding with the period of NMDA receptor hypersensitivity, transient

C. Ikonomidou, F. Bosch, M. Miksa, P. Bittigau, J. Vöckler, V. Stefovskaja, Department of Pediatric Neurology, Charité-Virchow Clinics, Humboldt University, Augustenburger Platz 1, 13353 Berlin, Germany. K. Dikranian, T. I. Tenkova, J. W. Olney, Department of Psychiatry, Washington University School of Medicine, 4940 Children's Place, St. Louis, MO 63110, USA. L. Turski, Eisai London Research Laboratories, Bernard Katz Building, University College London, Gower Street, London WC1E 6BT, UK.

*To whom correspondence should be addressed: E-mail: hrissanthi.ikonomidou@charite.de

REPORTS

blockade of NMDA receptors triggers a wave of apoptotic neurodegeneration in which large numbers of neurons are deleted

from the developing brain.

Seven-day-old rats were injected intraperitoneally (ip) with vehicle or dizocilpine

[(+)]MK801 (0.5 mg per kilogram of body weight) at 0, 8, and 16 hours and the brains examined at 24 hours by TUNEL (terminal deoxynucleotidyl transferase-mediated dUTP nick-end labeling) and silver staining to detect degenerating cells (6, 7). In the vehicle-treated rats, degenerating neurons were sparsely distributed in the forebrain (Fig. 1, A and C, and Table 1). In contrast, in (+)MK801-treated rats there was a marked increase of degenerating neurons in specific regions (Fig. 1, B and D, and Table 1). Using an unbiased optical dissector method (8), we determined that MK801 caused an increased numerical density of degenerating neurons from 3-fold in the hypothalamus to 39-fold in the laterodorsal thalamus (Table 1). The density of degenerating neurons in vehicle-treated rats varied from 0.2 to 1.55% of the total neuronal density in the brain regions examined, whereas in (+)MK801-treated pups the density of degenerating neurons was as high as 15 to 26% of the total neuronal density in layer II of parietal, frontal, and cingulate cortices and 12% in the laterodorsal thalamus (Table 1). Examination of the degenerating cells by electron microscopy (9) revealed (Fig. 1, F and G) that the degenerative process was ultrastructurally indistinguishable from the physiological (programmed) cell death that occurs naturally in the developing brain (10, 11).

To determine whether nonneuronal cells were vulnerable to the proapoptotic effect of (+)MK801, we used TUNEL staining in combination with immunohistochemistry for glial fibrillary acidic protein (GFAP) to identify astrocytes (12). Examination of histological sections from 7-day-old rats treated with (+)MK801 revealed that cells staining positive for GFAP were distinct from those staining positive for TUNEL. Apoptotic cells that were examined by electron microscopy in the early stages of degeneration retained the morphological characteristics of neurons.

Administration of (+)MK801 (0.25 to 1

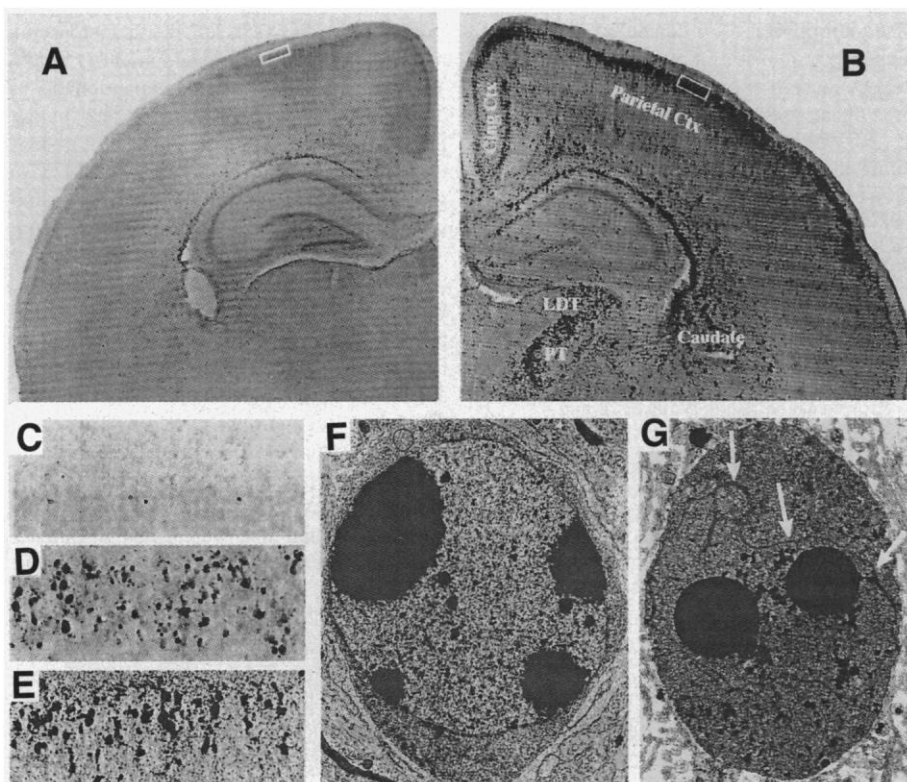
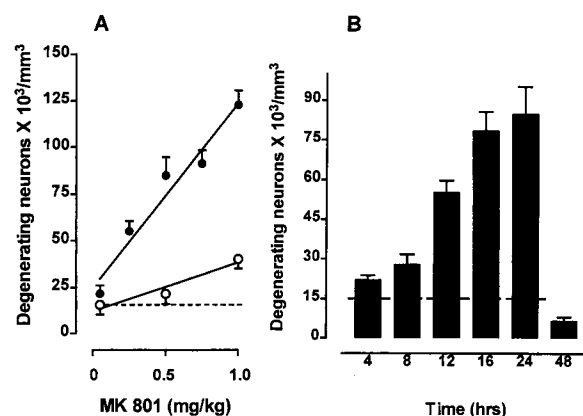


Fig. 1. (A and B) Low-magnification ($\times 9.8$) images of transverse hemisections from the brains of 8-day-old rats treated with vehicle (A) or (+)MK801 (B) 24 hours previously. Both sections were stained by the TUNEL method. TUNEL-positive neurons (small dark dots) are abundant in the brain of the (+)MK801-treated rat (B), but present in insignificant amounts in the vehicle-treated control (A). (C) Enlargement ($\times 98$) of the boxed region in (A). (D) Enlargement ($\times 98$) of the boxed region in (B). (E) Magnified view ($\times 98$) of the superficial parietal cortex of an 8-day-old rat 24 hours after PCP treatment, showing that PCP triggers the same apoptotic response as (+)MK801 in layer II neurons of the parietal cortex. (E) was stained by the DeOlmos silver method (7) and shows that this silver method stains the same populations of degenerating neurons as the TUNEL method in the immature brain after PCP or (+)MK801 treatment. (F and G) Electron micrographs of degenerating neurons in (B). Ultrastructural changes after (+)MK801 treatment are similar to those seen in neurons undergoing programmed cell death (10, 11). (F) Early stage of apoptosis. (G) A later stage in which the cell is more condensed and the nuclear membrane (arrows) has become fragmented and discontinuous. Throughout both stages the plasma membrane remains intact. Magnification, $\times 3275$.

Fig. 2. (A) The effect of dose on the apoptotic response to (+)MK801 (●) or (-)MK801 (○) was studied by administering a single dose of (+)MK801 (0.05, 0.25, 0.5, 0.75, or 1 mg/kg ip) or (-)MK801 (0.05, 0.5, or 1 mg/kg ip) on P7 and killing the rat pups 24 hours later ($n = 5$ to 7). Degenerating neurons were sampled by the optical dissector method (8) in silver-stained brain sections to provide a numerical density (degenerating neurons per cubic millimeter) for each of the 16 brain regions designated in Table 1. The numerical density counts from these brain regions were added to give a cumulative density count of degenerating neurons for each brain, and a mean was calculated for each treatment condition. Analysis of variance (ANOVA) revealed a significant effect of treatment with (+)MK801 [$F(5,26) = 53.97$; $P < 0.0001$] with multiple comparisons showing that a dose of 0.05 mg of (+)MK801 per kilogram did not trigger apoptosis, whereas doses >0.25 mg/kg significantly increased apoptosis. Treatment of rat pups with (-)MK801 on P7 resulted in a weak neurodegenerative response that became significant compared with vehicle-treated rats (dashed line) only at the dose of 1 mg/kg. (B) The time course of the apoptosis response to (+)MK801 was studied by administering a single dose of (+)MK-801 (0.5 mg/kg ip) on P7 and killing the rat pups 4, 8, 12, 16, 24, or 48 hours later. The apoptotic response was evaluated as described in (A). ANOVA revealed a significant effect of posttreatment interval on severity of brain damage [$F(6,28) = 34.43$; $P < 0.0001$], with multiple comparisons showing significant increase at 4 hours and a more robust response at 16 and 24 hours. By 48 hours there were no remaining signs of apoptosis. Dashed line indicates spontaneous apoptosis.



REPORTS

mg/kg ip) triggered apoptotic neurodegeneration in the 7-day-old rat brain that was dose-dependent (Fig. 2A). Rat pups that were killed at 4, 8, 12, 16, 24, and 48 hours after (+)MK801 (0.5 mg/kg) treatment showed an apoptotic response at 4 hours that increased progressively in the 12- to 24-hour interval (Fig. 2B).

To determine whether the proapoptotic

effect of MK801 can be attributed to its NMDA receptor-blocking activity, we administered the NMDA antagonists phenylcyclidine (PCP), ketamine, and carboxypiperazin-4-yl-propyl-1-phosphonic acid (CPP). When administered by dosing regimens calculated to maintain a steady blockade of NMDA receptors for at least 8 hours (13), all three agents induced a pattern of cell degen-

eration similar to that induced by (+)MK801 (Tables 1 and 2 and Fig. 1, E and F). Electron microscopy verified that the degenerative reaction induced by each agent was ultrastructurally indistinguishable from the programmed cell death that occurs naturally during brain development (10, 11). We also tested the (-) enantiomer of MK801, which is substantially less potent than (+)MK801 in blocking NMDA receptors. At a dose of 1 mg/kg, (-)MK801 triggered a weak apoptotic response compared with the same dose of (+)MK801 (Fig. 2A).

We administered either vehicle or (+)MK801 to rats on postnatal days 0 (P0), P3, P7, P14, or P21. In addition, we treated pregnant rats on embryonic day 17 (E17), E19, or E21 with (+)MK801 [0.5 mg/kg subcutaneously (sc) at 0, 8, and 16 hours]. This dose regimen was chosen because it produced a maximal apoptotic response in our initial experiments with 7-day-old rats. Fetuses (removed by hysterotomy on E18 or E20) or postnatal pups were killed at 24 hours after the first treatment of the mother with (+)MK801.

Between P0 and P14, (+)MK801 triggered apoptosis, but the magnitude of the response was dependent on the developmental age (Tables 1 and 2). Sensitivity to (+)MK801-induced apoptosis was high on both P0 and P3, increased between P3 and P7, and then decreased sharply between P7 and P14. On P21 apoptotic neurons were undetectable in vehicle-treated rats and detectable at very low levels in (+)MK801-treated rats.

Distinct patterns of apoptotic neurodegeneration were observed at different developmental ages (Table 2). The rate of spontane-

Table 1. The NMDA antagonist (+)MK801 increases the rate of apoptosis in the brain of 8-day-old rats. Seven-day-old rats received either vehicle or (+)MK801 (0.5 mg/kg ip) at 0, 8, and 16 hours and were killed at 24 hours on postnatal day 8 (P8). By use of an optical dissector method (8), the numerical cell densities (cells per cubic millimeter) and degenerating cell densities (degenerating cells per cubic millimeter) in 16 brain regions of vehicle- and (+)MK801-treated rats (*n* = 5 to 7) were estimated. Shown are numerical cell densities (mean ± SEM) in vehicle-treated 8-day-old rats. The extent of apoptosis in vehicle-treated and (+)MK801-treated rats is shown as the ratio of degenerating cell density to total cell density and is expressed as a percentage (mean ± SEM). ***p* < 0.01, ****p* < 0.001 (Student's *t* test). CA1 HPC: CA1 hippocampus; DG: dentate gyrus; Thal ld: laterodorsal thalamus; Thal md: mediodorsal thalamus; Thal v: ventral thalamus; Hypothal vm: ventromedial hypothalamus; Fr: frontal cortex; Par: parietal cortex; Cing: cingulate cortex; Rspl: retrosplenial cortex; II, IV: layers 2 and 4.

Brain region	Vehicle		MK801
	Numerical cell density (total) (mean/mm ³ ± SEM)	Degenerating cells/total cell density (%) (mean ± SEM)	Degenerating cells/total cell density (%) (mean ± SEM)
CA1 HPC	220,050 ± 4,584	0.85 ± 0.11	3.35 ± 0.7***
DG	284,127 ± 23,089	0.37 ± 0.06	1.75 ± 0.3***
Subiculum	198,124 ± 8,205	0.59 ± 0.04	10.70 ± 1.7***
Caudate	242,534 ± 11,140	0.29 ± 0.04	4.77 ± 0.9***
Thal ld	133,945 ± 13,148	0.30 ± 0.05	11.91 ± 2.2***
Thal md	199,335 ± 6,398	0.40 ± 0.01	2.39 ± 0.3***
Thal v	132,907 ± 2,634	0.76 ± 0.05	2.77 ± 0.7**
Hypothal vm	134,500 ± 2,343	0.90 ± 0.01	2.98 ± 0.7**
Fr II	219,432 ± 4,541	1.55 ± 0.18	22.65 ± 1.9***
Fr IV	142,120 ± 10,323	0.20 ± 0.05	1.43 ± 0.2***
Par II	223,900 ± 13,434	1.08 ± 0.28	26.13 ± 2.5***
Par IV	156,078 ± 6,323	0.22 ± 0.05	1.72 ± 0.3***
Cing II	218,932 ± 11,239	1.54 ± 0.21	15.49 ± 1.8***
Cing IV	148,100 ± 6,125	0.13 ± 0.03	3.22 ± 0.9***
Rspl II	235,948 ± 13,857	0.89 ± 0.07	11.49 ± 1.8***
Rspl IV	143,250 ± 10,857	0.33 ± 0.08	5.95 ± 0.4***

Table 2. NMDA antagonists trigger an increased rate of apoptosis in the rat brain on P0, P3, or P7. At these ages rat pups received either vehicle or (+)MK801 (0.5 mg/kg ip) at 0, 8, and 16 hours and were killed at 24 hours. The proapoptotic effect of PCP, ketamine, or CPP was tested in 7-day-old rats. Drugs were administered according to the dosing regimen described in (13). By use of an optical disector method (8), the numerical densities of degenerating neurons (degenerating neurons per cubic millimeter) in 14 brain regions of vehicle- and MK801-treated pups were estimated. Shown are mean

numerical densities of degenerating neurons ± SEM (*n* = 5 to 7). Effects of NMDA antagonists on the rate of apoptosis at each age are presented as ratios of mean numerical densities of degenerating cells in drug-treated versus age-matched vehicle-treated rats [expressed as fold increase (↑)]. NMDA antagonists do not trigger apoptosis in brain regions displaying no physiological apoptosis, and vulnerability to the proapoptotic action of NMDA antagonists is dependent on developmental age. **p* < 0.05, ***p* < 0.01, ****p* < 0.001 (Student's *t* test). Abbreviations as in Table 1.

Brain region	Numerical density of degenerating neurons (means/mm ³ ± SEM)								
	P0			P3			P7		
	Vehicle	MK801 (fold ↑)		Vehicle	MK801 (fold ↑)		PCP (fold ↑)	Ketamine (fold ↑)	CPP (fold ↑)
CA1 HPC	3,786 ± 305	21,648 ± 1,917** (5.7)	4,576 ± 756	20,107 ± 1,690*** (4.4)	1,863 ± 242	7,180 ± 1,549*** (3.9)	6,998 ± 110*** (3.8)	6,649 ± 1,161*** (3.6)	7,200 ± 1,553*** (3.9)
DG	4,796 ± 716	83,786 ± 1,397*** (17.4)	2,745 ± 420	14,288 ± 1,043*** (5.2)	1,045 ± 170	4,990 ± 978*** (4.8)	4,733 ± 518*** (4.5)	3,181 ± 860*** (3.0)	2,221 ± 239*** (2.1)
Subiculum	3,996 ± 459	25,589 ± 2,331*** (6.4)	3,663 ± 760	29,266 ± 3,048*** (8.0)	1,168 ± 172	21,199 ± 3,368*** (18.0)	20,872 ± 3,173*** (18.0)	22,572 ± 4,194*** (19.3)	22,591 ± 2,762*** (19.3)
Caudate	8,349 ± 915	36,790 ± 3,207*** (4.4)	4,359 ± 740	19,654 ± 1,268*** (4.5)	703 ± 97	11,569 ± 2,183*** (16.5)	10,514 ± 1,166*** (15.0)	8,285 ± 1,132*** (11.8)	4,811 ± 462*** (6.8)
Hypothal vm	23,186 ± 2,309	92,669 ± 20,285* (4.0)	1,835 ± 270	8,059 ± 987*** (4.4)	1,209 ± 14	4,008 ± 941*** (3.3)	4,577 ± 767** (4.0)	3,576 ± 452*** (3.0)	3,762 ± 508*** (3.1)
Thal ld	2,428 ± 423	4,756 ± 1,487 (2.0)	3,172 ± 756	31,555 ± 4,510*** (9.9)	402 ± 67	15,939 ± 2,944*** (39.7)	9,791 ± 3,433*** (24.4)	12,297 ± 2,142*** (30.9)	9,979 ± 1,381*** (24.8)
Thal md	18,824 ± 2,078	31,796 ± 2,804* (1.7)	926 ± 85	3,295 ± 414*** (3.6)	768 ± 20	4,598 ± 598** (6.0)	3,137 ± 82** (4.1)	3,914 ± 726** (5.1)	2,708 ± 330*** (3.5)
Thal v	10,787 ± 693	20,443 ± 2,700 (1.9)	1,156 ± 205	3,396 ± 582*** (3.0)	1,003 ± 66	3,682 ± 930*** (3.7)	2,666 ± 264*** (2.7)	3,886 ± 882*** (3.9)	3,098 ± 682*** (3.1)
Fr II	0	0 (-)	5,672 ± 750	33,412 ± 4,667*** (5.9)	3,398 ± 395	49,701 ± 4,169*** (14.6)	43,754 ± 5,210*** (12.9)	25,696 ± 2,175*** (7.6)	42,176 ± 4,452*** (12.4)
Par II	0	0 (-)	5,291 ± 905	34,286 ± 3,461*** (6.5)	2,421 ± 602	58,505 ± 5,555*** (24.2)	54,447 ± 7,405*** (22.5)	34,030 ± 6,796*** (14.1)	50,504 ± 2,784*** (20.9)
Cing II	0	0 (-)	9,242 ± 1200	11,548 ± 272 (1.3)	3,369 ± 445	33,913 ± 3,941*** (10.1)	28,513 ± 3,032*** (8.5)	18,736 ± 3,178*** (5.6)	25,002 ± 1,550*** (7.4)
Cing IV	0	0 (-)	3,065 ± 518	3,206 ± 63 (1.0)	196 ± 44	4,769 ± 1,332*** (24.8)	4,301 ± 544*** (21.9)	3,378 ± 674*** (17.2)	2,584 ± 178*** (13.2)
Rspl II	0	0 (-)	5,320 ± 445	6,009 ± 57 (1.1)	2,089 ± 159	27,110 ± 4,247*** (12.9)	24,353 ± 5,101*** (12.0)	19,710 ± 1,771*** (9.4)	17,424 ± 272*** (8.3)
Rspl IV	0	0 (-)	2,104 ± 482	2,287 ± 23 (1.1)	476 ± 115	8,523 ± 573*** (18.0)	6,405 ± 544*** (13.5)	4,309 ± 474*** (9.1)	3,471 ± 252*** (7.3)

ous apoptosis in vehicle-treated rats was high on P0, especially in the mediodorsal and ventral thalamic nuclei, the ventromedial hypothalamus, and caudate. Brain regions with an appreciable rate of spontaneous apoptosis on P0 also showed a robust response to MK801, which was most evident in the dentate gyrus (17-fold increase over the spontaneous rate). In contrast to all other brain regions studied, apoptosis was not detected in the cerebral cortex in either vehicle- or MK801-treated animals on P0. On P3 the rate of spontaneous apoptosis decreased markedly in the hypothalamus and mediodorsal and ventral thalamic nuclei, remained at a moderately high level in most other regions, and de novo increased to high levels in layer II of the frontal, parietal, cingulate, and retrosplenial divisions of the cerebral cortex. On P3, MK801 triggered apoptosis in all regions studied, notably the subiculum (8-fold) and laterodorsal thalamus (10-fold). On P7 the spontaneous rate declined to modest levels in all regions, but the MK801-induced increases remained high in many regions (14.6, 16.5, 18, 18, 24.2, 24.8, and 39.7 times the spontaneous rate in the frontal cortex, caudate, subiculum, retrosplenial, parietal, cingulate cortices, and laterodorsal thalamus, respectively). Regions that showed high spontaneous or induced rates on P0 (dentate gyrus, CA1 hippocampus, ventromedial hypothalamus, and ventral and mediodorsal thalamus) displayed low spontaneous and induced rates on P7.

The rate of (+)MK801-induced apoptosis in fetuses exposed in utero on E21 and killed on P0 (24 hours after the first treatment of the mother) was similar to that of animals treated as infants on P0 (27.3, 9.9, and 2.5 times higher than the spontaneous rate in the dentate gyrus, hippocampal CA1 subfield, and ventromedial hypothalamus, respectively). Fetuses exposed in utero on E19 showed no increases in regions examined, with the exception of the ventromedial hypothalamus (1.8-fold higher than vehicle-treated rats). Fetuses exposed in utero to either vehicle or MK801 on E17 showed neither spontaneous nor induced apoptosis in any of the regions examined.

To determine the specificity of the proapoptotic action of NMDA antagonists, we tested the effects of 6-nitro-7-sulfamoylbenzof[quinoxaline-2,3-dione (NBQX), an antagonist of non-NMDA glutamate receptors [20 mg/kg ip given at 0, 75, 150 min and 8 hours ($n = 5$)], and scopolamine hydrobromide, an antagonist of cholinergic muscarinic receptors [0.3 mg/kg ip given at 0, 4, and 8 hours ($n = 5$)]. In addition, we tested haloperidol, an antagonist of dopamine receptors [10 mg/kg ip given at 0 and 8 hours ($n = 5$)]. None of these agents reproduced the apoptosis-inducing action of NMDA antagonists.

Finally, because NMDA receptors are highly permeable to Ca^{2+} ions (13), we examined whether blockade of Ca^{2+} influx by other routes—that is, voltage-dependent Ca^{2+} channels—also cause apoptotic neurodegeneration in the brain. We treated 7-day-old rats with the Ca^{2+} -channel blockers (14) nimodipine (50 mg/kg at 0 and 8 hours; $n = 6$) or nifedipine (10 mg/kg at 0 and 8 hours; $n = 6$) and examined the brains by TUNEL and silver staining at 24 hours after treatment. Neither of these agents caused significant apoptosis in the 7-day-old rat brain.

Our findings indicate that in the developing rat brain transient blockade of NMDA receptors causes sensitive neurons to die by a process that resembles the programmed cell death that occurs naturally in the developing brain (10, 11). The effect is caused by NMDA receptor blockade because agents that block NMDA receptors by different mechanisms triggered the response. The effect is age-dependent and is specific for NMDA receptors because it was not reproduced by blockade of other major excitatory systems in the brain (muscarinic and non-NMDA glutamatergic) or by blockade of a major inhibitory system (dopaminergic). Thus, it appears that many neurons in the mammalian brain undergo a stage during development when they are critically dependent on glutamate stimulation through NMDA receptors, and sustained deprivation of this input activates programmed cell death.

The neuronal populations vulnerable to degeneration induced by NMDA antagonists have abundant NMDA receptors (15). However, receptor density is not the sole determinant of neuronal vulnerability, because neurons in the CA1 hippocampal region express high levels of mRNA for the NR1 receptor subunit (15) on P7 and at this age are less sensitive than cortical layer II neurons to the proapoptotic action of NMDA antagonists. However, on E21 and P0, CA1 neurons are more vulnerable than cerebrocortical neurons to NMDA antagonists, which suggests that additional factors, such as the stage in synaptogenesis and the subunit composition of the NMDA receptor assembly, may govern neuronal vulnerability.

NMDA antagonists were most effective in triggering apoptosis in the rat forebrain on P7, the age at which the rat forebrain is most vulnerable to the excitotoxic effect of NMDA (2). Thus, during this developmental period survival of NMDA receptor-bearing neurons depends on glutamatergic input being regulated within narrow bounds. In the human fetal forebrain, expression of NMDA receptors peaks during weeks 20 to 22 of gestation (16), a period that marks the beginning of the brain growth spurt, which spans much of the third trimester of pregnancy and overlaps extensively into the postnatal period (17). In the rat, peak expres-

sion of NR1 (15) and the brain growth spurt (18) occur in the first week after birth. If peak vulnerability of the human forebrain to the proapoptotic action of NMDA antagonists corresponds to these developmental events in the rat, the window of vulnerability for humans would include the entire third trimester of pregnancy. Our findings may have relevance in a human context of drug abuse, where fetuses may be exposed in utero to agents such as PCP (angel dust), ketamine (special K), and ethanol (18, 19), all potent NMDA antagonists. Furthermore, human infants are sometimes exposed to ketamine and nitrous oxide, two NMDA antagonists widely used in pediatric anesthesia (20, 21).

It is important to consider the length of time for which NMDA receptors must be blocked for the neurodegenerative process to become operative. The threshold dose of (+)MK801-induced apoptosis in our study was 0.25 mg/kg, which produced behavioral symptoms indicative of NMDA receptor blockade lasting 4 to 6 hours. An increased rate of apoptosis was detected in the infant rat brain beginning 4 hours after administration of a single dose of (+)MK801 (0.5 mg/kg). Thus, blockade of NMDA receptors for ~4 hours is sufficient to trigger apoptotic neurodegeneration in the developing mammalian brain.

Blockade of NMDA receptors gives rise to different patterns of neuronal loss depending on the stage of development at which the interference occurs. Such a mechanism could contribute to a variety of neuropsychiatric disorders.

References and Notes

- H. Komuro and P. Rakic, *Science* **260**, 95 (1993); L. Guerrini, F. Blasi, D. Denis-Donini, *Proc. Natl. Acad. Sci. U.S.A.* **92**, 9077 (1995).
- C. Ikonomidou, J. L. Mosinger, K. Shahid Salles, J. Labruyere, J. W. Olney, *J. Neurosci.* **9**, 2809 (1989).
- Y. Ben-Ari, R. Khazipov, X. Leinekugel, O. Caillard, J. L. Gaiarsa, *Trends Neurosci.* **20**, 523 (1997).
- R. Balazs, N. Hack, O. S. Jorgensen, *Int. J. Dev. Neurosci.* **8**, 347 (1990); G. M. Yan, B. Ni, K. A. Wood, S. M. Paul, *Brain Res.* **656**, 43 (1994).
- E. Gould, H. A. Cameron, B. S. McEwen, *J. Comp. Neurol.* **340**, 551 (1994).
- Y. Gavrieli, Y. Sherman, S. A. Ben-Sasson, *J. Cell Biol.* **119**, 493 (1992). In apoptotic cell death DNA undergoes internucleosomal cleavage into fragments that can be detected by tissue staining. TUNEL staining is not specific for apoptosis, but it can be used for identifying and mapping apoptotic neurons if apoptosis is confirmed by ultrastructural evaluation. For TUNEL staining the rats were deeply anesthetized and the brains perfused with fixative containing paraformaldehyde (4%) in phosphate buffer and embedded in paraffin. Brains were either sectioned into 70- μm -thick slices by vibratome or embedded in paraffin and sectioned into 10- μm -thick slices. Serial sections from the entire forebrain were stained by TUNEL (ApoTag) and counterstained with methyl green. Nuclei displaying DNA cleavage stained dark brown, surrounded by green cytoplasm.
- J. S. DeOlmos and W. R. Ingram, *Brain Res.* **33**, 523 (1971). DeOlmos cupric silver staining can be used to detect degenerating neurons that are dying by apoptotic or nonapoptotic mechanisms. We used this method to verify the distribution and numerical den-

sity of apoptotic cells identified by TUNEL. Both staining procedures produced the same pattern of degeneration in the brains of vehicle-treated rats and the same pattern of increased degeneration in the brains of (+)MK801-treated rats. To visualize degenerating cells by DeOlmos cupric silver staining, we perfused the brains with fixative containing paraformaldehyde (4%) in phosphate buffer, and serial transverse sections (70 μ m thick) were cut by vibratome from the entire forebrain and stained with silver nitrate and cupric nitrate. Degenerating cells incorporate silver and appear dark against a light background.

8. Neuronal degeneration was quantified in 16 brain regions (Table 1) using the optical disector and fractionator method as described [L. L. Cruz-Orive and E. R. Weibel, *Am. J. Physiol.* **258**, L148 (1990)]. A counting frame (0.05 mm by 0.05 mm, disector height 0.07 mm), and a high-aperture objective were used for visualizing and counting neurons. Unbiased sampling of each brain region was performed by randomly selecting 8 to 10 viewing fields over which the counting frame was positioned for counting at different focal levels by the optical disector method. The numerical density of normal neurons in any given region was determined by counting neuronal profiles in 70- μ m-thick sections stained with a Nissl stain (methylene blue, azure II). The numerical density of degenerating neurons in any given region was determined by counting argyrophilic profiles in 70- μ m-thick sections stained by the DeOlmos silver method (7). Counting was performed in a blinded manner.
9. C. Charriaut-Marlangue and Y. Ben-Ari, *Neuroreport* **7**, 61 (1995); B. Grasl-Kraupp et al., *Hepatology* **21**, 1465 (1995).
10. A. H. Wyllie, J. F. R. Kerr, A. R. Currie, *Int. Rev. Cytol.* **68**, 251 (1980).
11. M. J. Ishimaru, C. Ikonomidou, K. Dikranian, J. W. Olney, *Soc. Neurosci. Abstr.* **23**, 895 (1997). Physiological cell death (PCD), an example of apoptosis, occurs naturally in the developing central nervous system. In the fetal rat brain, with the exception of germinal matrix zones where apoptosis is frequent, apoptotic neurons are confined primarily to lower brain centers. In the early neonatal period (P1 to P5) apoptotic profiles become increasingly abundant throughout many non-germinal matrix regions of the midbrain and forebrain. By P7, PCD has largely run its course and apoptotic profiles are not found in high concentration in any forebrain region.
12. Double labeling for GFAP and TUNEL was performed by first staining sections by TUNEL (6), washing them thoroughly at room temperature in a solution of 0.01 M phosphate-buffered saline (PBS)-Triton X-100 (0.5%), and incubating them for 1 hour in the same solution with 1% bovine serum albumin. The sections were then incubated overnight at 4°C in the presence of monoclonal antibody against GFAP (1:400 dilution; G3893, Sigma). After PBS rinses, sections were incubated with goat antibody to mouse immunoglobulin G (IgG) (1:200; BODIPY, Molecular Probes) in PBS-Triton X-100 for 1 hour at room temperature. Microscopic fields were photographed with a Kodak digital camera under fluorescence illumination to detect localization of the BODIPY fluorescence probe and under ordinary illumination to detect the TUNEL diaminobenzidine reaction product. The two images from a given field were then superimposed with Photoshop software to determine whether the GFAP and TUNEL labels were colocalized in the same cells.
13. MK801 remains detectable in the rodent brain or cerebrospinal fluid for 3 to 4 hours after systemic administration. Elimination half-life of MK801 in rats was estimated to be 1.9 hours. The drug reaches maximal concentrations in the brain within 10 to 30 min after administration [A. Vezzani et al., *J. Pharmacol. Exp. Ther.* **249**, 278 (1989)]. Phencyclidine (PCP), which freely penetrates blood-brain barriers, has a plasma elimination half-life of 3.9 hours and an even longer half-life in the rat brain [J. L. Valentine, L. W. Arnold, S. M. Owens, *J. Pharmacol. Exp. Ther.* **269**, 1079 (1994)]. A single dose of PCP (10 mg/kg ip) was used because it produces behavioral symptoms indicative of NMDA receptor blockade lasting for 8 to 10 hours in 7-day-old rats. Ketamine freely penetrates the brain but is excret-

- ed rapidly and has a short half-life in the brain [P. F. White, M. P. Marietta, C. R. Pudwill, W. L. Way, A. J. Trevor, *J. Pharmacol. Exp. Ther.* **196**, 545 (1976)]. It was administered in a series of seven injections spaced evenly over 9 hours, each injection delivering a dose of 20 mg/kg sc. CPP penetrates blood-brain barriers poorly but has a long half-life in the brain [J. D. Kristensen, P. Hartvig, R. Karlsten, T. Gordh, M. Halldin, *Br. J. Anaesth.* **74**, 193 (1995)]. To maintain a steady blockade of NMDA receptors for 8 hours, we administered CPP at a dose of 15 mg/kg ip at 0, 50, and 100 min and at 4 and 8 hours. Rat pups were killed at 24 hours after the first treatment.
14. I. Izquierdo et al., *Trends Pharmacol. Sci.* **11**, 309 (1990); A. C. Kappelle et al., *Br. J. Pharmacol.* **108**, 780 (1993).
15. H. Monyer, N. Burnashev, D. J. Laurie, B. Sakmann, P. H. Seeburg, *Neuron* **12**, 529 (1994); C. Akazawa, R. Shigemoto, Y. Bessho, S. Nakanishi, N. Mizuno, *J. Comp. Neurol.* **347**, 150 (1994).
16. H. Lee and B. H. Choi, *Exp. Neurol.* **118**, 284 (1992); J. Zhong, D. P. Carrozza, K. Williams, D. B. Pritchett, P. B. Molinoff, *J. Neurochem.* **64**, 531 (1995).
17. J. Dobbing and J. Sands, *Early Hum. Dev.* **3**, 79 (1979); J. D. Reynolds and J. F. Brien, *Can. J. Physiol. Pharmacol.* **73**, 1209 (1995); L. S. Meyer, L. E. Kotch, E. P. Riley, *Alcohol. Clin. Exp. Res.* **14**, 23 (1990).

18. D. M. Lovinger, G. White, F. F. Weight, *Science* **243**, 1721 (1989); P. L. Hoffman, C. S. Rabe, F. Moses, B. Tabakoff, *J. Neurochem.* **52**, 1937 (1989).
19. K. L. Jones and D. W. Smith, *Lancet* **ii**, 999 (1973); C. D. Coles, I. E. Smith, A. Falek, *Adv. Alcohol Subst. Abuse* **6**, 87 (1987). Intrauterine exposure of the human fetus to ethanol results in microcephaly and a syndrome of neurobehavioral deficits referred to as fetal alcohol syndrome. It is thought that the neurobehavioral deficits result primarily from a deleterious effect of ethanol during fetal development in late pregnancy.
20. D. L. Reich and G. Silvey, *Can. J. Anaesth.* **36**, 186 (1989); P. F. White, W. L. Way, A. J. Trevor, *Anesthesiology* **56**, 119 (1982).
21. V. Jevtovic-Todorovic et al., *Nature Med.* **4**, 460 (1998). Nitrous oxide (laughing gas) is an NMDA antagonist at concentrations relevant to its use as an anesthetic.
22. Supported in part by BMBF grant 01K095151 and grants from the National Institute of Aging (AG 11355), the National Institute of Drug Abuse (DA 05072), and the Research Scientist Award from the National Institute of Mental Health (MH 38894) to J.W.O.

26 August 1998; accepted 17 November 1998

Role of Heteromer Formation in GABA_B Receptor Function

Rohini Kuner, Georg Köhr, Sylvia Grünewald, Gisela Eisenhardt, Alfred Bach, Hans-Christian Kornau*

Recently, GBR1, a seven-transmembrane domain protein with high affinity for γ -aminobutyric acid (GABA)_B receptor antagonists, was identified. Here, a GBR1-related protein, GBR2, was shown to be coexpressed with GBR1 in many brain regions and to interact with it through a short domain in the carboxyl-terminal cytoplasmic tail. Heterologously expressed GBR2 mediated inhibition of adenylyl cyclase; however, inwardly rectifying potassium channels were activated by GABA_B receptor agonists only upon coexpression with GBR1 and GBR2. Thus, the interaction of these receptors appears to be crucial for important physiological effects of GABA and provides a mechanism in receptor signaling pathways that involve a heterotrimeric GTP-binding protein.

GABA_B receptors play a critical role in the fine-tuning of central nervous system synaptic transmission (1) and are attractive targets for the treatment of epilepsy, anxiety, depression, cognitive deficits, and nociceptive disorders (2). Their effects are brought about by multiple signaling cascades involving adenylyl cyclase, inwardly rectifying potassium channels (GIRKs), and voltage-dependent Ca²⁺ channels (1). Recently, the cDNA for a seven-transmembrane domain (7TM) protein, termed GABA_B receptor 1 (GBR1), which exists in two NH₂-terminal splice forms (A and B) and has high affinity for GABA_B

receptor antagonists, was identified. GBR1 can account for some, but not all, of the functional properties of native GABA_B receptors (3).

We used the yeast two-hybrid system (Y2H) (4) to look for intracellular proteins that mediate signaling events downstream of GBR1 activation. The COOH-terminal intracellular region of GBR1 (amino acids 857 to 960 in GBR1A) (3) was used as a bait (5) to screen a rat brain cDNA library (6). Our search through 2 \times 10⁶ recombinant clones yielded five positive clones, all of which encoded overlapping fragments of the COOH-terminus of a previously unidentified protein. Full-length cloning (7) of the identified cDNA revealed an open reading frame for a protein of 940 amino acids with an NH₂-terminal 40-residue signal sequence and seven internal hydrophobic segments characteristic for 7TM proteins (Fig. 1A) (8). A public database search for related sequences (8) revealed GBR1B with the best score (36%

R. Kuner, S. Grünewald, G. Eisenhardt, A. Bach, H.-C. Kornau, BASF-LYNX Bioscience AG, Department of Neuroscience, Im Neuenheimer Feld 515, D-69120 Heidelberg, Germany. G. Köhr, Max-Planck-Institute for Medical Research, Department of Molecular Neurobiology, Jahnstrasse 29, D-69120 Heidelberg, Germany.

*To whom correspondence should be addressed. E-mail: kornau@basf-lynx.de